Crystal structure, synthesis and thermal properties of tetrakis(4-benzoylpyridine-κN)bis(isothiocyanato-κN)iron(II)

Carsten Wellm* and Christian Näther

Institut für Anorganische Chemie, Universität Kiel, Max-Eyth. Str. 2, 241128 Kiel, Germany. *Correspondence e-mail: cwellm@ac.uni-kiel.de

The asymmetric unit of the title compound, [Fe(NCS)$_2$(C$_{12}$H$_9$NO)$_4$], consists of an Fe^{II} ion that is located on a centre of inversion, as well as two 4-benzoylpyridine ligands and one thiocyanate anion in general positions. The Fe^{II} ions are coordinated by two N-terminal-bonded thiocyanate anions and four 4-benzoylpyridine ligands into discrete complexes with a slightly distorted octahedral geometry. These complexes are further linked by weak C—H···O hydrogen bonds into chains running along the c-axis direction. Upon heating, this complex loses half of the 4-benzoylpyridine ligands and transforms into a compound with the composition Fe(NCS)$_2$(4-benzoylpyridine)$_2$, that might be isotypic to the corresponding Mn^{II} compound and for which the structure is unknown.

1. Chemical context

Coordination compounds based on thio- or selenocyanate anions have attracted much interest in recent years because of their luminescence behavior and their versatile magnetic properties (Mekuimemba et al., 2018; Palion-Gazda et al., 2015, 2017; Mautner et al., 2016a,b; Näther et al., 2013). For the latter, compounds are of special interest in which paramagnetic transition-metal cations are linked by the anionic ligands into 1D or 2D coordination polymers. Some of them show single-chain-magnet behavior (Wöhlert et al., 2013; 2014a; Mautner et al., 2018), others are ferromagnets (Suckert et al., 2016) and in a few cases the critical temperature can be tuned by mixed-crystal formation (Neumann et al., 2018a, 2019; Wellm et al., 2018).

However, in most cases compounds are obtained from solution in which the anionic ligands are only terminally N-bonded, which frequently leads to the formation of discrete complexes (Mautner et al., 2015, 2017). These compounds can be transformed into coordination polymers by thermal decomposition, in which some of the co-ligands are irreversibly removed (Näther et al., 2013), leading to the formation of polymorphic or isomeric modifications (Wöhlert et al., 2014b). In several cases Mn^{II}, Fe^{II}, Co^{II}, Ni^{II} and Cd^{II} compounds behave similarly but in others, different modifications are obtained depending on the actual metal cation.

This is the case e.g. for thiocyanate complexes with 4-benzoylpyridine as co-ligand. The discrete complexes with the composition M(NCS)$_2$(4-benzoylpyridine)$_4$ (M = Co and Ni) transform into isotypic chain compounds with the composition [M(NCS)$_2$(4-benzoylpyridine)$_2$]$_n$, whereas both the Mn and Cd compounds each form a different crystalline

OPEN ACCESS

917
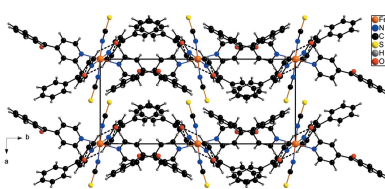
phase (Neumann *et al.*, 2018*b*; Wellm & Näther, 2018). Therefore, we became interested in the corresponding complex with Fe^{II} to check if this compound could also transform into a 4-benzoylpyridine-deficient phase and if this phase would be isotypic to that with Mn^{II}, Co^{II} or Cd^{II}. The synthesis of the title compound can easily be achieved by the reaction of Fe(Cl)$_2$·4H$_2$O and K(SCN)$_2$ with 4-benzoylpyridine, leading to the formation of phase pure samples (see Figure S1 in the supporting information). Upon heating, two mass losses are observed, of which the first one is in agreement with that expected for the removal of half of the 4-benzoylpyridine co-ligands (Figure S2). If the residue formed after the first thermogravimetric step is investigated by XRPD, it is obvious that a crystalline phase is formed (Figure S3) that is not isotypic to [M(NCS)$_2$(4-benzoylpyridine)$_2$]$_n$ (M = Co, Cd) but very similar to that of Mn(NCS)$_2$(4-benzoylpyridine)$_2$ (Rams *et al.*, 2017; Neumann *et al.*, 2018*b*; Wellm & Näther, 2018). Additionally, IR spectra show that the residue exhibits bridging μ-1,3-coordinating thiocyanate anions, in contrast to the terminal thiocyanate anions of the title compound (Figure S4). Unfortunately, as is the case for the Mn^{II} compound, the powder pattern cannot be indexed and no single crystals can be obtained. Therefore, the structure of this compound is still unknown.
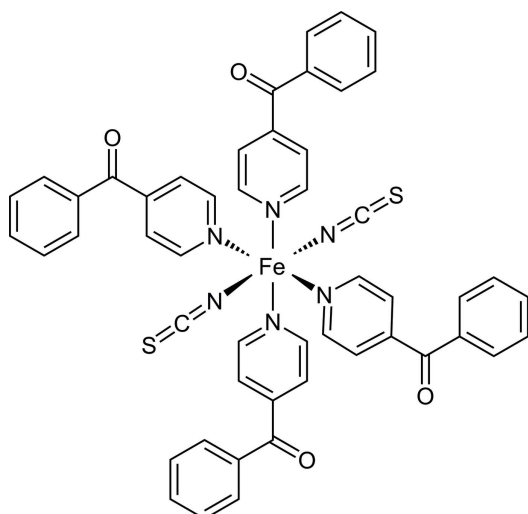
2. Structural commentary

The crystal structure of the title compound (Fig. 1) is isotypic to the corresponding Co^{II}, Ni^{II}, Mn^{II}, Zn^{II} and Cd^{II} compounds (Drew *et al.*, 1985; Soliman *et al.*, 2014; Wellm & Näther, 2018; Neumann *et al.*, 2018*b*). The asymmetric unit consists of one N-bonded terminal thiocyanate anion and two crystallographically independent 4-benzoylpyridine ligands in general positions, as well as of one Fe^{II} cation located on a centre of inversion (Fig. 1). The Fe^{II} ions are sixfold coordinated by the pyridine N-atoms of the four neutral 4-benzoylpyridine ligands and the N atoms of the two terminal thiocyanate anions. The Fe—N bonds to the 4-benzoylpyridine coligands, ranging between 2.2576 (13) and 2.2597 (13) Å, are significantly longer than those to the anionic ligands of

Table 1
Selected geometric parameters (Å, °).

Fe1—N1	2.0982 (14)	Fe1—N31	2.2597 (13)
Fe1—N11	2.2576 (13)		
N1^{i}—Fe1—N11	88.79 (5)	N1—Fe1—N31	89.79 (5)
N1—Fe1—N11	91.21 (5)	N11—Fe1—N31	88.15 (5)
N1^{i}—Fe1—N31	90.21 (5)	N11^{i}—Fe1—N31	91.85 (5)

Symmetry code: (i) $-x, -y + 1, -z + 1$.

2.0982 (14) Å (Table 1) and correspond to those observed in the isotypic compounds [M(NCS)$_2$(C$_{12}$H$_9$NO)$_4$] (M = Mn, Co, Ni, Zn, Cd; Wellm & Näther, 2018; Drew *et al.*, 1985; Soliman *et al.*, 2014; Neumann *et al.*, 2018*b*). The N—M—N angles deviate from the ideal values, which shows that the octahedra are slightly distorted in agreement with the values for the angle variance (1.8) and the quadratic elongation (1.003) (Robinson *et al.*, 1971). Furthermore, the pyridine and phenyl rings of the 4-benzoylpyridine ligands are not co-planar to the carbonyl plane. The dihedral angle between the pyrdine ring (N11/C11–15) and the carbonyl plane (C13/C16/C17/O11) amounts to 35.24 (10)°, while the one between the carbonyl plane (C13/C16/C17/O11) and the phenyl ring (C17–C22) is 24.23 (8)°. The corresponding values for the second 4-benzoylpyrdine ligand are 35.69 (9)° between the pyridine ring (N31/C31–C35) and the carbonyl plane (C33/C36/C37/O21) and 23.79 (9)° between the carbonyl plane (C33/C36/C37/O21) and the phenyl ring (C37–C42). Additionally, there are weak intramolecular C—H···N interactions between the thiocyanate atoms N1 and N1^{i} and aromatic hydrogen atoms
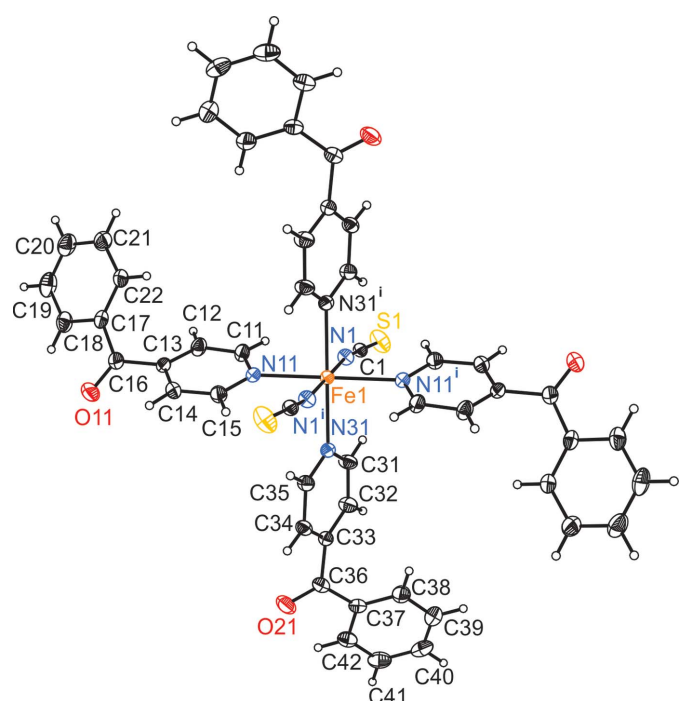

Figure 1
View of a discrete complex with the atom labeling and displacement ellipsoids drawn at the 50% probability level. Symmetry code: (i) $-x, -y + 1, -z + 1$.

Table 2
Hydrogen-bond geometry (Å, °).

$D-H\cdots A$	$D-H$	$H\cdots A$	$D\cdots A$	$D-H\cdots A$
C11—H11···N1	0.95	2.51	3.136 (2)	123
C15—H15···N1[i]	0.95	2.57	3.134 (2)	118
C15—H15···O21[ii]	0.95	2.57	3.293 (2)	133
C31—H31···N1	0.95	2.60	3.168 (2)	119
C35—H35···N1[i]	0.95	2.52	3.125 (2)	121
C35—H35···O21[ii]	0.95	2.61	3.309 (2)	131

Symmetry codes: (i) $-x, -y + 1, -z + 1$; (ii) $-x, -y + 1, -z + 2$.

H11, H31, H15 and H35 that might contribute to the stabilization of the complexes (Table 2).

3. Supramolecular features

The discrete complexes are connected by relatively weak C—H···O hydrogen bonds between the C—H hydrogen atoms and the atom O21($-x, 1 - y, 2 - z$) of a symmetry-related 4-benzoylpyridine ligand, forming 12-membered rings that are located on centres of inversion (Fig. 2 and Table 2). Atom O21 acts as acceptor for two hydrogen bonds from C15—H15 and C35—H35; thus each complex is connected by four hydrogen bonds to two additional symmetry-equivalent complexes, leading to the formation of chains that extend along the c-axis direction (Figs. 2 and 3 and Table 2). There are no further directed interactions observed between the chains (Fig. 3).

4. Database survey

There are several crystal structures reported in the Cambridge Structure Database (Version 5.40, last update February 2018; Groom *et al.*, 2016) that consist of transition-metal cations, thiocyanate anions and 4-benzoylpyrine. In most of these compounds, the metal cations are octahedrally coordinated. Three of them are coordination polymers in which the cations are connected by pairs of μ-1,3-coordinating thiocyanate anions, with the 4-benzoylpyridine ligands being perpendicular to the elongation axis of the chain (Neumann *et al.*, 2018b; Rams *et al.*, 2017; Jochim *et al.*, 2018). The other
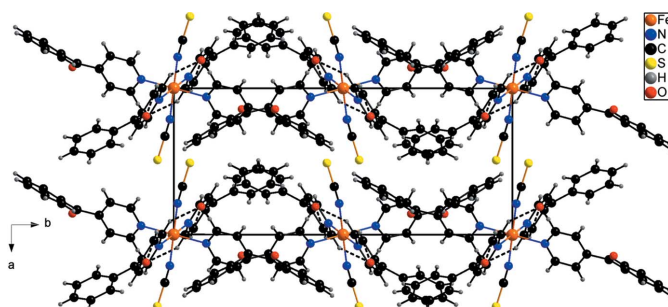

Figure 3
Crystal packing of the title compound viewed along the crystallographic c axis with intermolecular C—H···O hydrogen bonds (Table 2) shown as dashed lines.

octahedral compounds are either discrete complexes with only 4-benzoylpyridine as neutral co-ligand, isotypic to the title compound and of the general composition $M(NCS)_2$(4-benzoylpyridine)$_4$ ($M = Co^{II}, Ni^{II}, Mn^{II}, Zn^{II}$ and Cd^{II}; Drew *et al.*, 1985; Soliman *et al.*, 2014; Wellm & Näther, 2018; Neumann *et al.*, 2018b), or solvates that are built up of two terminally N-bonded thiocyanates, two 4-benzoylpyridine ligands and acetonitrile (Suckert *et al.*, 2017b) or methanol as solvent (Suckert *et al.*, 2017a; Wellm & Näther, 2019). Additionally, there is a quadratic planar Cu^{II} complex (Bai *et al.*, 2011) and a tetrahedral Zn^{II} complex (Neumann *et al.*, 2018b) in which the metal cation is coordinated by two terminally N-bonded thiocyanates and two 4-benzoylpyridine ligands.

5. Synthesis and crystallization

Fe(Cl)$_2$·4H$_2$O and K(SCN)$_2$ were purchased from Merck and 4-benzoylpyridine was purchased from Alfa Aesar.

Synthesis:

Crystals of the title compound suitable for single crystal X-ray diffraction were obtained within three days by the reaction of 59.6 mg Fe(Cl)$_2$·4H$_2$O (0.3 mmol) and 58.3 mg (0.6 mmol) K(SCN)$_2$ with 27.5 mg 4-benzoylpyridine (0.15 mmol) in ethanol (1.5 mL), followed by slow evaporation of the solvent.
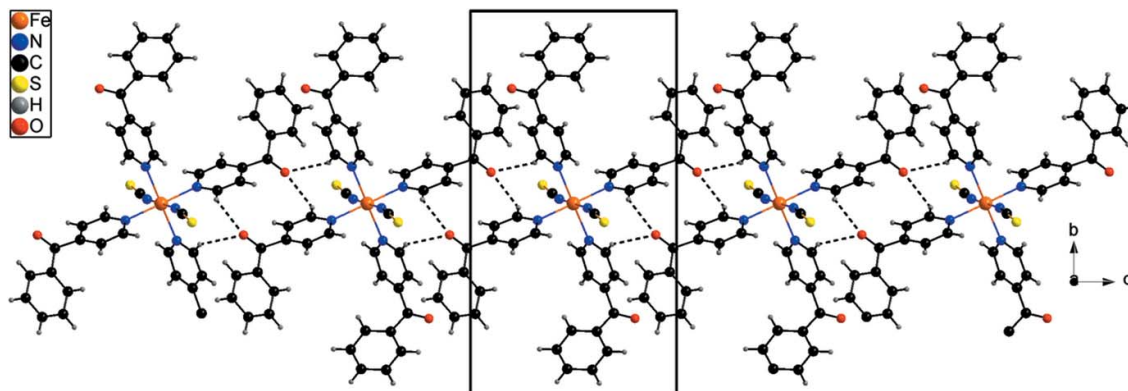

Figure 2
Crystal packing of the title compound viewed along the crystallographic a axis with intermolecular C—H···O hydrogen bonds (Table 2) shown as dashed lines.

Table 3
Experimental details.

Crystal data	
Chemical formula	$[Fe(NCS)_2(C_{12}H_9NO)_4]$
M_r	904.82
Crystal system, space group	Monoclinic, $P2_1/c$
Temperature (K)	200
a, b, c (Å)	9.0610 (6), 20.9844 (11), 11.2527 (9)
β (°)	90.526 (9)
V (Å³)	2139.5 (2)
Z	2
Radiation type	Mo $K\alpha$
μ (mm⁻¹)	0.51
Crystal size (mm)	$0.16 \times 0.04 \times 0.03$
Data collection	
Diffractometer	STOE IPDS1
Absorption correction	Numerical (X-SHAPE and X-RED32; Stoe, 2008)
T_{min}, T_{max}	0.817, 0.965
No. of measured, independent and observed $[I > 2\sigma(I)]$ reflections	25216, 4907, 4090
R_{int}	0.060
$(\sin\theta/\lambda)_{max}$ (Å⁻¹)	0.650
Refinement	
$R[F^2 > 2\sigma(F^2)]$, $wR(F^2)$, S	0.044, 0.113, 1.04
No. of reflections	4907
No. of parameters	287
H-atom treatment	H-atom parameters constrained
$\Delta\rho_{max}$, $\Delta\rho_{min}$ (e Å⁻³)	0.50, −0.51

Computer programs: X-AREA (Stoe, 2008), XP in SHELXTL and SHELXS97 (Sheldrick, 2008), SHELXL2014 (Sheldrick, 2015), DIAMOND (Brandenburg, 1999) and publCIF (Westrip, 2010).

Experimental details:

Differential thermal analysis-thermogravimetric (DTA-TG) measurements were performed in a dynamic nitrogen atmosphere in Al_2O_3 crucibles using an STA PT1600 thermobalance from Linseis. The XRPD measurements were performed by using a Stoe transmission powder diffraction system (STADI P) with Cu $K\alpha$ radiation that was equipped with a linear, position-sensitive MYTHEN detector from Stoe & Cie. The IR data were measured using a Bruker Alpha-P ATR-IR spectrometer.

6. Refinement

Crystal data, data collection and structure refinement details are summarized in Table 3. Hydrogen atoms were positioned with idealized geometry (C—H = 0.95 Å) and were refined using a riding model with $U_{iso}(H) = 1.2U_{eq}(C)$.

References

Bai, Y., Zheng, G.-S., Dang, D.-B., Zheng, Y.-N. & Ma, P.-T. (2011). *Spectrochim. Acta A*, **79**, 1338–1344.

Brandenburg, K. (1999). *DIAMOND*. Crystal Impact GbR, Bonn, Germany.

Drew, M. G. B., Gray, N. I., Cabral, M. F. & Cabral, J. de O. (1985). *Acta Cryst.* C**41**, 1434–1437.

Groom, C. R., Bruno, I. J., Lightfoot, M. P. & Ward, S. C. (2016). *Acta Cryst.* B**72**, 171–179.

Jochim, A., Rams, M., Neumann, T., Wellm, C., Reinsch, H., Wójtowicz, G. M. & Näther, C. (2018). *Eur. J. Inorg. Chem.* pp. 4779–4789.

Mautner, F. A., Berger, C., Fischer, R. & Massoud, S. S. (2016*a*). *Inorg. Chim. Acta*, **448**, 34–41.

Mautner, F. A., Berger, C., Fischer, R. C. & Massoud, S. S. (2016*b*). *Inorg. Chim. Acta*, **439**, 69–76.

Mautner, F. A., Fischer, R. C., Rashmawi, L. G., Louka, F. R. & Massoud, S. S. (2017). *Polyhedron*, **124**, 237–242.

Mautner, F. A., Scherzer, M., Berger, C., Fischer, R. C., Vicente, R. & Massoud, S. S. (2015). *Polyhedron*, **85**, 20–26.

Mautner, F. A., Traber, M., Fischer, R. C., Torvisco, A., Reichmann, K., Speed, S., Vicente, R. & Massoud, S. S. (2018). *Polyhedron*, **154**, 436–442.

Mekuimemba, C. D., Conan, F., Mota, A. J., Palacios, M. A., Colacio, E. & Triki, S. (2018). *Inorg. Chem.* **57**, 2184–2192.

Näther, C., Wöhlert, S., Boeckmann, J., Wriedt, M. & Jess, I. (2013). *Z. Anorg. Allg. Chem.* **639**, 2696–2714.

Neumann, T., Jess, I., dos Santos Cunha, C., Terraschke, H. & Näther, C. (2018*b*). *Inorg. Chim. Acta*, **478**, 15–24.

Neumann, T., Rams, M., Tomkowicz, Z., Jess, I. & Näther, C. (2019). *Chem. Commun.* **55**, 2652–2655.

Neumann, T., Rams, M., Wellm, C. & Näther, C. (2018*a*). *Cryst. Growth Des.* **18**, 6020–6027.

Palion-Gazda, J., Gryca, I., Maroń, A., Machura, B. & Kruszynski, R. (2017). *Polyhedron*, **135**, 109–120.

Palion-Gazda, J., Machura, B., Lloret, F. & Julve, M. (2015). *Cryst. Growth Des.* **15**, 2380–2388.

Rams, M., Tomkowicz, Z., Böhme, M., Plass, W., Suckert, S., Werner, J., Jess, I. & Näther, C. (2017). *Phys. Chem. Chem. Phys.* **19**, 3232–3243.

Robinson, K., Gibbs, G. V. & Ribbe, P. H. (1971). *Science*, **172**, 567–570.

Sheldrick, G. M. (2008). *Acta Cryst.* A**64**, 112–122.

Sheldrick, G. M. (2015). *Acta Cryst.* C**71**, 3–8.

Soliman, S. M., Elzawy, Z. B., Abu-Youssef, M. A. M., Albering, J., Gatterer, K., Öhrström, L. & Kettle, S. F. A. (2014). *Acta Cryst.* B**70**, 115–125.

Stoe (2008). *X-AREA*, *X-RED32* and *X-SHAPE*. Stoe & Cie, Darmstadt, Germany.

Suckert, S., Rams, M., Böhme, M., Germann, L. S., Dinnebier, R. E., Plass, W., Werner, J. & Näther, C. (2016). *Dalton Trans.* **45**, 18190–18201.

Suckert, S., Rams, M., Rams, M. R. & Näther, C. (2017*a*). *Inorg. Chem.* **56**, 8007–8017.

Suckert, S., Werner, J., Jess, I. & Näther, C. (2017*b*). *Acta Cryst.* E**73**, 365–368.

Wellm, C. & Näther, C. (2018). *Acta Cryst.* E**74**, 1899–1902.

Wellm, C. & Näther, C. (2019). *Acta Cryst.* E**75**, 299–303.

Wellm, C., Rams, M., Neumann, T., Ceglarska, M. & Näther, C. (2018). *Cryst. Growth Des.* **18**, 3117–3123.

Westrip, S. P. (2010). *J. Appl. Cryst.* **43**, 920–925.

Wöhlert, S., Fic, T., Tomkowicz, Z., Ebbinghaus, S. G., Rams, M., Haase, W. & Näther, C. (2013). *Inorg. Chem.* **52**, 12947–12957.

Wöhlert, S., Runčevski, T., Dinnebier, R., Ebbinghaus, S. & Näther, C. (2014*b*). *Cryst. Growth Des.* **14**, 1902–1913.

Wöhlert, S., Tomkowicz, Z., Rams, M., Ebbinghaus, S. G., Fink, L., Schmidt, M. U. & Näther, C. (2014*a*). *Inorg. Chem.* **53**, 8298–8310.

supporting information

Crystal structure, synthesis and thermal properties of tetrakis(4-benzoyl-pyridine-*κN*)bis(isothiocyanato-*κN*)iron(II)

Carsten Wellm and Christian Näther

Computing details

Data collection: *X-AREA* (Stoe, 2008); cell refinement: *X-AREA* (Stoe, 2008); data reduction: *X-AREA* (Stoe, 2008); program(s) used to solve structure: *SHELXS97* (Sheldrick, 2008); program(s) used to refine structure: *SHELXL2014* (Sheldrick, 2015); molecular graphics: *XP* in *SHELXTL* (Sheldrick, 2008) and *DIAMOND* (Brandenburg, 1999); software used to prepare material for publication: *publCIF* (Westrip, 2010).

Tetrakis(4-benzoylpyridine-*κN*)bis(isothiocyanato-*κN*)iron(II)

Crystal data
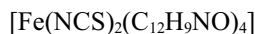
[Fe(NCS)$_2$(C$_{12}$H$_9$NO)$_4$]	$F(000) = 936$
$M_r = 904.82$	$D_x = 1.405$ Mg m^{-3}
Monoclinic, $P2_1/c$	Mo $K\alpha$ radiation, $\lambda = 0.71073$ Å
$a = 9.0610$ (6) Å	Cell parameters from 25216 reflections
$b = 20.9844$ (11) Å	$\theta = 2.5–27.5°$
$c = 11.2527$ (9) Å	$\mu = 0.51$ mm^{-1}
$\beta = 90.526$ (9)°	$T = 200$ K
$V = 2139.5$ (2) Å^3	Needle, light yellow
$Z = 2$	$0.16 \times 0.04 \times 0.03$ mm

Data collection

STOE IPDS-1 diffractometer	4907 independent reflections
	4090 reflections with $I > 2\sigma(I)$
φ scans	$R_{int} = 0.060$
Absorption correction: numerical (X-SHAPE and X-RED32; Stoe, 2008)	$\theta_{max} = 27.5°$, $\theta_{min} = 2.5°$
	$h = -11 \rightarrow 11$
$T_{min} = 0.817$, $T_{max} = 0.965$	$k = -27 \rightarrow 27$
25216 measured reflections	$l = -14 \rightarrow 14$

Refinement

Refinement on F^2	H-atom parameters constrained
Least-squares matrix: full	$w = 1/[\sigma^2(F_o^2) + (0.0769P)^2 + 0.3118P]$
$R[F^2 > 2\sigma(F^2)] = 0.044$	where $P = (F_o^2 + 2F_c^2)/3$
$wR(F^2) = 0.113$	$(\Delta/\sigma)_{max} < 0.001$
$S = 1.04$	$\Delta\rho_{max} = 0.50$ e Å^{-3}
4907 reflections	$\Delta\rho_{min} = -0.51$ e Å^{-3}
287 parameters	Extinction correction: SHELXL,
0 restraints	Fc*=kFc[1+0.001xFc$^2\lambda^3$/sin(2θ)]$^{-1/4}$
Hydrogen site location: inferred from neighbouring sites	Extinction coefficient: 0.026 (2)

Special details

Geometry. All esds (except the esd in the dihedral angle between two l.s. planes) are estimated using the full covariance matrix. The cell esds are taken into account individually in the estimation of esds in distances, angles and torsion angles; correlations between esds in cell parameters are only used when they are defined by crystal symmetry. An approximate (isotropic) treatment of cell esds is used for estimating esds involving l.s. planes.

Fractional atomic coordinates and isotropic or equivalent isotropic displacement parameters (Å^2)

	x	*y*	*z*	U_{iso}*/U_{eq}
Fe1	0.0000	0.5000	0.5000	0.01655 (12)
N1	0.21274 (16)	0.51129 (6)	0.43099 (13)	0.0221 (3)
C1	0.32862 (18)	0.52598 (7)	0.39685 (14)	0.0204 (3)
S1	0.48986 (5)	0.54766 (3)	0.34977 (5)	0.03812 (15)
N11	0.05996 (15)	0.40356 (6)	0.57514 (12)	0.0204 (3)
C11	0.18068 (19)	0.37360 (7)	0.53597 (16)	0.0248 (3)
H11	0.2429	0.3953	0.4819	0.030*
C12	0.2190 (2)	0.31228 (8)	0.57078 (17)	0.0270 (4)
H12	0.3043	0.2924	0.5393	0.032*
C13	0.13182 (19)	0.28026 (7)	0.65168 (15)	0.0224 (3)
C14	0.0108 (2)	0.31223 (8)	0.69739 (15)	0.0255 (3)
H14	−0.0487	0.2927	0.7562	0.031*
C15	−0.02230 (19)	0.37287 (8)	0.65646 (15)	0.0246 (3)
H15	−0.1068	0.3938	0.6871	0.030*
C16	0.1689 (2)	0.21450 (8)	0.69528 (16)	0.0288 (4)
C17	0.2345 (2)	0.16681 (7)	0.61300 (16)	0.0252 (4)
C18	0.3114 (2)	0.11520 (9)	0.66334 (19)	0.0319 (4)
H18	0.3276	0.1133	0.7468	0.038*
C19	0.3635 (2)	0.06699 (9)	0.5907 (2)	0.0393 (5)
H19	0.4160	0.0322	0.6246	0.047*
C20	0.3395 (2)	0.06935 (9)	0.4693 (2)	0.0400 (5)
H20	0.3751	0.0360	0.4202	0.048*
C21	0.2638 (2)	0.11996 (9)	0.41879 (19)	0.0367 (4)
H21	0.2475	0.1212	0.3353	0.044*
C22	0.2112 (2)	0.16913 (8)	0.49028 (16)	0.0286 (4)
H22	0.1599	0.2041	0.4556	0.034*
O11	0.1429 (2)	0.20092 (7)	0.79860 (13)	0.0537 (5)
N31	0.07705 (15)	0.54355 (6)	0.67343 (12)	0.0206 (3)
C31	0.2025 (2)	0.57704 (8)	0.68418 (15)	0.0274 (4)
H31	0.2607	0.5831	0.6153	0.033*
C32	0.2519 (2)	0.60332 (9)	0.79080 (16)	0.0277 (4)
H32	0.3403	0.6276	0.7937	0.033*
C33	0.17005 (18)	0.59348 (7)	0.89320 (14)	0.0217 (3)
C34	0.04162 (19)	0.55810 (8)	0.88302 (15)	0.0239 (3)
H34	−0.0168	0.5500	0.9511	0.029*
C35	−0.00132 (19)	0.53446 (8)	0.77268 (15)	0.0232 (3)
H35	−0.0904	0.5107	0.7672	0.028*
C36	0.21784 (19)	0.61552 (8)	1.01527 (15)	0.0252 (3)
C37	0.29466 (19)	0.67775 (8)	1.03193 (15)	0.0242 (3)

C38	0.2782 (2)	0.72793 (9)	0.95250 (17)	0.0335 (4)
H38	0.2207	0.7224	0.8822	0.040*
C39	0.3458 (3)	0.78642 (9)	0.9755 (2)	0.0383 (5)
H39	0.3335	0.8208	0.9214	0.046*
C40	0.4306 (2)	0.79423 (9)	1.07696 (19)	0.0363 (4)
H40	0.4772	0.8340	1.0923	0.044*
C41	0.4480 (2)	0.74438 (10)	1.15663 (18)	0.0372 (4)
H41	0.5067	0.7500	1.2262	0.045*
C42	0.3800 (2)	0.68632 (9)	1.13492 (16)	0.0309 (4)
H42	0.3913	0.6523	1.1900	0.037*
O21	0.19095 (18)	0.58129 (7)	1.10006 (12)	0.0400 (3)

Atomic displacement parameters (Å^2)

	U^{11}	U^{22}	U^{33}	U^{12}	U^{13}	U^{23}
Fe1	0.01555 (17)	0.01668 (16)	0.01743 (17)	−0.00085 (10)	0.00129 (12)	−0.00031 (11)
N1	0.0182 (7)	0.0252 (6)	0.0229 (7)	0.0000 (5)	0.0008 (5)	0.0007 (5)
C1	0.0222 (8)	0.0205 (7)	0.0183 (7)	0.0020 (6)	−0.0022 (6)	0.0004 (6)
S1	0.0200 (2)	0.0558 (3)	0.0387 (3)	−0.00491 (19)	0.00399 (19)	0.0148 (2)
N11	0.0235 (7)	0.0174 (6)	0.0201 (6)	0.0003 (5)	−0.0002 (5)	−0.0009 (5)
C11	0.0256 (8)	0.0194 (7)	0.0294 (9)	0.0008 (6)	0.0058 (7)	0.0008 (6)
C12	0.0267 (9)	0.0205 (7)	0.0340 (9)	0.0041 (6)	0.0060 (7)	0.0000 (7)
C13	0.0282 (8)	0.0174 (7)	0.0217 (8)	−0.0004 (6)	−0.0032 (6)	−0.0011 (6)
C14	0.0306 (9)	0.0236 (8)	0.0225 (8)	−0.0013 (6)	0.0032 (7)	0.0027 (6)
C15	0.0243 (8)	0.0245 (8)	0.0250 (8)	0.0024 (6)	0.0042 (6)	0.0013 (6)
C16	0.0381 (10)	0.0224 (8)	0.0257 (8)	0.0001 (7)	−0.0038 (7)	0.0026 (6)
C17	0.0260 (8)	0.0177 (7)	0.0318 (9)	−0.0011 (6)	−0.0020 (7)	0.0024 (6)
C18	0.0300 (9)	0.0259 (8)	0.0398 (11)	0.0019 (7)	−0.0070 (8)	0.0071 (7)
C19	0.0299 (10)	0.0269 (9)	0.0610 (14)	0.0106 (7)	0.0012 (9)	0.0075 (9)
C20	0.0395 (11)	0.0279 (9)	0.0527 (13)	0.0067 (8)	0.0126 (10)	−0.0018 (8)
C21	0.0459 (12)	0.0281 (9)	0.0362 (10)	0.0045 (8)	0.0086 (9)	−0.0008 (8)
C22	0.0358 (10)	0.0212 (7)	0.0290 (9)	0.0031 (6)	0.0008 (7)	0.0033 (6)
O11	0.1029 (15)	0.0328 (7)	0.0256 (7)	0.0158 (8)	0.0054 (8)	0.0069 (6)
N31	0.0232 (7)	0.0191 (6)	0.0194 (7)	−0.0018 (5)	0.0016 (5)	−0.0012 (5)
C31	0.0299 (9)	0.0330 (9)	0.0193 (8)	−0.0106 (7)	0.0052 (7)	−0.0038 (6)
C32	0.0270 (9)	0.0338 (9)	0.0224 (8)	−0.0118 (7)	0.0020 (7)	−0.0033 (7)
C33	0.0252 (8)	0.0209 (7)	0.0189 (7)	0.0012 (6)	−0.0006 (6)	−0.0003 (6)
C34	0.0261 (8)	0.0266 (7)	0.0189 (7)	−0.0017 (6)	0.0043 (6)	0.0006 (6)
C35	0.0221 (8)	0.0260 (8)	0.0215 (8)	−0.0044 (6)	0.0019 (6)	−0.0011 (6)
C36	0.0263 (9)	0.0303 (8)	0.0189 (8)	0.0010 (6)	0.0001 (6)	0.0003 (6)
C37	0.0240 (8)	0.0290 (8)	0.0194 (8)	0.0012 (6)	0.0010 (6)	−0.0042 (6)
C38	0.0422 (11)	0.0304 (9)	0.0278 (9)	−0.0002 (8)	−0.0076 (8)	−0.0024 (7)
C39	0.0482 (12)	0.0274 (9)	0.0394 (11)	−0.0012 (8)	0.0007 (9)	−0.0014 (8)
C40	0.0321 (10)	0.0359 (10)	0.0409 (11)	−0.0051 (8)	0.0077 (8)	−0.0161 (8)
C41	0.0305 (10)	0.0503 (11)	0.0309 (10)	−0.0052 (8)	−0.0041 (8)	−0.0124 (8)
C42	0.0315 (10)	0.0387 (10)	0.0224 (8)	0.0001 (7)	−0.0033 (7)	−0.0033 (7)
O21	0.0545 (9)	0.0444 (8)	0.0210 (6)	−0.0136 (7)	−0.0015 (6)	0.0055 (6)

Geometric parameters (Å, º)

Fe1—N1ⁱ	2.0982 (14)	C20—H20	0.9500
Fe1—N1	2.0982 (14)	C21—C22	1.395 (3)
Fe1—N11	2.2576 (13)	C21—H21	0.9500
Fe1—N11ⁱ	2.2576 (13)	C22—H22	0.9500
Fe1—N31	2.2597 (13)	N31—C31	1.341 (2)
Fe1—N31ⁱ	2.2597 (13)	N31—C35	1.343 (2)
N1—C1	1.163 (2)	C31—C32	1.391 (2)
C1—S1	1.6237 (17)	C31—H31	0.9500
N11—C11	1.340 (2)	C32—C33	1.392 (2)
N11—C15	1.349 (2)	C32—H32	0.9500
C11—C12	1.388 (2)	C33—C34	1.384 (2)
C11—H11	0.9500	C33—C36	1.509 (2)
C12—C13	1.384 (2)	C34—C35	1.389 (2)
C12—H12	0.9500	C34—H34	0.9500
C13—C14	1.388 (2)	C35—H35	0.9500
C13—C16	1.502 (2)	C36—O21	1.221 (2)
C14—C15	1.385 (2)	C36—C37	1.491 (2)
C14—H14	0.9500	C37—C38	1.388 (3)
C15—H15	0.9500	C37—C42	1.399 (2)
C16—O11	1.222 (2)	C38—C39	1.395 (3)
C16—C17	1.491 (2)	C38—H38	0.9500
C17—C22	1.396 (3)	C39—C40	1.380 (3)
C17—C18	1.404 (2)	C39—H39	0.9500
C18—C19	1.386 (3)	C40—C41	1.386 (3)
C18—H18	0.9500	C40—H40	0.9500
C19—C20	1.383 (3)	C41—C42	1.386 (3)
C19—H19	0.9500	C41—H41	0.9500
C20—C21	1.383 (3)	C42—H42	0.9500
N1ⁱ—Fe1—N1	180.0	C19—C20—H20	119.8
N1ⁱ—Fe1—N11	88.79 (5)	C21—C20—H20	119.8
N1—Fe1—N11	91.21 (5)	C20—C21—C22	120.1 (2)
N1ⁱ—Fe1—N11ⁱ	91.21 (5)	C20—C21—H21	119.9
N1—Fe1—N11ⁱ	88.79 (5)	C22—C21—H21	119.9
N11—Fe1—N11ⁱ	180.0	C21—C22—C17	119.71 (17)
N1ⁱ—Fe1—N31	90.21 (5)	C21—C22—H22	120.1
N1—Fe1—N31	89.79 (5)	C17—C22—H22	120.1
N11—Fe1—N31	88.15 (5)	C31—N31—C35	116.99 (14)
N11ⁱ—Fe1—N31	91.85 (5)	C31—N31—Fe1	123.01 (11)
N1ⁱ—Fe1—N31ⁱ	89.79 (5)	C35—N31—Fe1	119.96 (11)
N1—Fe1—N31ⁱ	90.21 (5)	N31—C31—C32	123.48 (16)
N11—Fe1—N31ⁱ	91.85 (5)	N31—C31—H31	118.3
N11ⁱ—Fe1—N31ⁱ	88.15 (5)	C32—C31—H31	118.3
N31—Fe1—N31ⁱ	180.00 (7)	C31—C32—C33	119.05 (16)
C1—N1—Fe1	170.93 (13)	C31—C32—H32	120.5
N1—C1—S1	179.08 (15)	C33—C32—H32	120.5

C11—N11—C15	117.19 (14)	C34—C33—C32	117.73 (15)
C11—N11—Fe1	119.46 (11)	C34—C33—C36	118.27 (15)
C15—N11—Fe1	123.32 (11)	C32—C33—C36	123.88 (15)
N11—C11—C12	123.01 (16)	C33—C34—C35	119.59 (15)
N11—C11—H11	118.5	C33—C34—H34	120.2
C12—C11—H11	118.5	C35—C34—H34	120.2
C13—C12—C11	119.53 (16)	N31—C35—C34	123.15 (15)
C13—C12—H12	120.2	N31—C35—H35	118.4
C11—C12—H12	120.2	C34—C35—H35	118.4
C12—C13—C14	117.79 (15)	O21—C36—C37	120.89 (16)
C12—C13—C16	122.26 (16)	O21—C36—C33	118.27 (16)
C14—C13—C16	119.87 (16)	C37—C36—C33	120.84 (14)
C15—C14—C13	119.35 (16)	C38—C37—C42	119.42 (17)
C15—C14—H14	120.3	C38—C37—C36	122.42 (16)
C13—C14—H14	120.3	C42—C37—C36	118.07 (16)
N11—C15—C14	123.00 (16)	C37—C38—C39	120.24 (18)
N11—C15—H15	118.5	C37—C38—H38	119.9
C14—C15—H15	118.5	C39—C38—H38	119.9
O11—C16—C17	121.05 (16)	C40—C39—C38	119.87 (19)
O11—C16—C13	118.74 (17)	C40—C39—H39	120.1
C17—C16—C13	120.21 (15)	C38—C39—H39	120.1
C22—C17—C18	119.72 (17)	C39—C40—C41	120.32 (18)
C22—C17—C16	122.25 (15)	C39—C40—H40	119.8
C18—C17—C16	117.80 (17)	C41—C40—H40	119.8
C19—C18—C17	119.70 (19)	C40—C41—C42	120.11 (18)
C19—C18—H18	120.1	C40—C41—H41	119.9
C17—C18—H18	120.1	C42—C41—H41	119.9
C20—C19—C18	120.35 (18)	C41—C42—C37	120.03 (18)
C20—C19—H19	119.8	C41—C42—H42	120.0
C18—C19—H19	119.8	C37—C42—H42	120.0
C19—C20—C21	120.41 (19)		

Symmetry code: (i) −*x*, −*y*+1, −*z*+1.

Hydrogen-bond geometry (Å, °)

D—H···*A*	*D*—H	H···*A*	*D*···*A*	*D*—H···*A*
C11—H11···N1	0.95	2.51	3.136 (2)	123
C15—H15···N1[i]	0.95	2.57	3.134 (2)	118
C15—H15···O21[ii]	0.95	2.57	3.293 (2)	133
C31—H31···N1	0.95	2.60	3.168 (2)	119
C35—H35···N1[i]	0.95	2.52	3.125 (2)	121
C35—H35···O21[ii]	0.95	2.61	3.309 (2)	131

Symmetry codes: (i) −*x*, −*y*+1, −*z*+1; (ii) −*x*, −*y*+1, −*z*+2.